New insights into the environmental factors controlling the circumpolar ground thermal regime

Olli Karjalainen[1], Miska Luoto[2], Juha Aalto[2,3], and Jan Hjort[1]

[1]Geography Research Unit, University of Oulu, FI-90014, Oulu, Finland
[2]Department of Geosciences and Geography, University of Helsinki, FI-00014, Helsinki, Finland
[3]Finnish Meteorological Institute, FI-00101, Helsinki, Finland

Correspondence to: Olli Karjalainen (olli.karjalainen@oulu.fi)

Abstract. The thermal state of permafrost affects Earth surface systems and human activity in the Arctic and has implications to global climate. Improved understanding of the local-scale variability in the circumpolar ground thermal regime is required to account for its sensitivity to changing climatic and geoecological conditions. Here, we statistically related circumpolar observations of mean annual ground temperature (MAGT) and active-layer thickness (ALT) to high-resolution (~1 km^2) geospatial data of climatic and local environmental conditions. The aim was to characterize the relative importance of key environmental factors and the magnitude and direction of their effects in predicting the circumpolar ground thermal regime at 1-km scale. The multivariate models fitted well to MAGT and ALT observations with average R^2 values being ~0.94 and 0.78, respectively. Corresponding predictive performances in terms of root mean square error were ~1.31 °C and 87 cm. Freezing air temperatures was the main factor controlling MAGT in permafrost conditions while thawing temperatures dominated when permafrost was not present. ALT was most strongly related to solar radiation and precipitation with important non-linear influences from soil properties. Our findings suggest that in addition to climatic factors, local-scale variability in soil and topography need to be considered in order to realistically assess the current and future ground thermal regimes across the circumpolar region.

1 Introduction

In the face of changing Arctic, it is crucial to understand the mechanisms that drive the current geocryological dynamics of the region. Thaw of permafrost is expected to significantly attribute to hydrological and geoecological alterations in landscapes (Jorgenson et al., 2013; Liljedahl et al., 2016). In addition, greenhouse gas emissions from thawing permafrost soils have a potential to affect the global climate system (e.g. Grosse et al., 2016). Permafrost temperature and the depth of the overlying seasonally thawed layer, i.e. active layer, are key components of the ground thermal regime that govern various geomorphological and ecological processes (Frauenfeld et al., 2007; Aalto et al., 2017), as well as human activity in permafrost regions (Callaghan et al., 2011; Vincent et al., 2017). Outside the permafrost domain, extensive regions undergo seasonal freezing, which in itself affects many aspects of natural and human activities (e.g. Shiklomanov, 2012; Westermann et al., 2015).

Climatic conditions account for large-scale spatial variation in mean annual ground temperature (MAGT) and active-layer thickness (ALT) (Bonnaventure and Lamoureux, 2013; Streletskiy et al., 2015; Westermann et al., 2015). From regional to local scales, topography-induced solar radiation input (Etzelmüller, 2013) and intercepting layers of snow, soil and vegetation mediate their effect (e.g. Osterkamp, 2007; Fisher et al., 2016; Gruber et al., 2017; Aalto et al., 2018a; Zhang et al., 2018). Winter temperatures have been suggested to be most important for permafrost temperature (Smith and Riseborough, 1996; Etzelmüller et al., 2011), while ALT is essentially dependent on summer temperatures (Oelke et al., 2003; Melnikov et al., 2004; Luo et al., 2016). In wintertime, snow layer insulates the ground from cold air causing an offset, i.e. ground is warmer than air (e.g. Aalto et al., 2018b; Zhang et al., 2018). Water precipitation alters the thermal conductivity of near-surface layers

through its control on, e.g., soil water balance (Smith and Riseborough, 1996; Callaghan et al., 2011; Marmy et al., 2013). Arguably, the responsiveness of the circumpolar ground thermal regime to atmospheric forcing also depends on its initial thermal state. In permafrost conditions, temperature changes are lagged by the higher demand of energy for phase changes of water in the active layer (i.e. latent-heat exchange), whereas in temperate soils climate signal affects more directly (Romanovsky et al., 2010; Kurylyk et al., 2014). In addition to the effect of ground ice content on heat transfer, its development is an important geomorphic factor (e.g. Liljedahl et al., 2016).

Improved knowledge on circumpolar permafrost dynamics is required to understand various geoecological interactions and feedbacks associated with warming Arctic (e.g. Wu et al., 2012; Grosse et al., 2016; Yi et al., 2018). Such information is useful for climate change assessments (Zhang et al., 2005, Smith et al., 2009), infrastructure design and maintenance, as well as for adaptation to changing conditions (Romanovsky et al., 2010, Streletskiy et al., 2015). Physically based ground thermal models can account for various biogeophysical processes acting in vegetation, snow and soil layers (e.g. Lawrence and Swenson, 2011) but are not applicable at high spatial resolutions over large areas owing to their tedious model parameterizations (Chadburn et al., 2017). For example, commonly used circumpolar 0.5° latitude/longitude resolution has been considered insufficient in characterizing spatial variation in soil properties and vegetation, thus leading to large mismatch between the simulations and observations (Park et al., 2013). Recently, Peng et al. (2018) assessed spatio-temporal long-term trends in circumpolar ALT with a large observational dataset stressing that ALT strongly depends on local topo-edaphic factors (e.g. Harlan and Nixon, 1978) and that thorough analyses of environmental factors controlling ALT at varying scales are urgently required.

Here, we use a statistical modelling framework employing multiple algorithms from regression to machine learning to examine the factors contributing to the spatial variation in the circumpolar ground thermal regime. More specifically, we aim to (1) calibrate realistic models of MAGT and ALT (the responses) utilizing geospatial data on climatic and local conditions (the predictors) across the Northern Hemisphere land areas, and (2) examine the nature of the contributing factors in both permafrost and non-permafrost conditions using circumpolar field observations of MAGT and ALT. The analyses provide detailed insights into the importance of key environmental factors and the magnitudes and direction of their effect at 1-km resolution.

2 Methods

2.1 Study area and observational data

We compiled MAGT and ALT observations from the period 2000–2014 over the Northern Hemisphere land areas north of the 30th parallel (Fig.1). To examine possible differences in the contribution of environmental factors between permafrost and non-permafrost conditions we used two separate MAGT datasets; observed MAGT at or below 0 °C, i.e. permafrost, ($MAGT_{\leq 0\,°C}$, n = 469) and above 0 °C ($MAGT_{>0\,°C}$, n = 315). For each MAGT and ALT site, averages over the study period were then calculated from available annual averages or suitable single measurements. The observations were standardized by requiring that MAGT was recorded at or near the depth of zero annual amplitude (ZAA) where annual temperature variation was less than 0.1 °C, and that ALT (n = 298) values represented the maximum thaw depth of a given year based on mechanical probing or derived from ground temperature measurements or thaw tubes (Brown et al., 2000; Aalto et al., 2018a). When ZAA depth was not reported or not retrievable from numeric data, we used the value at the depth of 15 m, where annual temperature fluctuation in most conditions is negligible (see French, 2007), although in thermally highly diffusive subsurface materials, such as bedrock, the depth can be greater (e.g. Throop et al. 2012). With some MAGT observations, ZAA depth was reportedly not reached but we chose to include these cases assuming that annual means calculated from year-round records from one or multiple years were representative of long-term thermal state. MAGT measured at less than two meters below the surface were excluded unless reported to be at the depth of ZAA.

The Global Terrestrial Network for Permafrost database (GTN-P, Biskaborn et al., 2015) was the principal constituent of our datasets (~60 % of MAGT and ~67 % of ALT observations). Additionally, data were gathered from open Internet databases (e.g. Roshydromet, meteo.ru; Natural Resources Canada, GEOSCAN database; National Geothermal Data System) and previous studies to cover a maximal range of climatological and environmental conditions (see Table S1 and S2 for sources)

A minimum geopositional location precisions of two decimal degrees (~1,110 m at the Equator) for MAGT and a commonly used arc minute (~1,800 m) for often less accurately geopositioned ALT sites were adopted both to ascertain adequate spatial match with geospatial data layers and to moderate the need to exclude lower precision observations. Nonetheless, almost 90 % of MAGT and more than two-thirds of ALT observations had a precision of at least three decimal degrees (~110 m at the Equator). Further exclusions were made when the ground thermal regime was evidently disturbed by recent forest fire, anthropogenic heat source, large water bodies or the effect of geothermal heat in temperature-depth curve (Jorgenson et al., 2010; Woo, 2012) as revealed by source data or cartographical examination of the site.

2.2 Predictor variables

Nine geospatial predictors representing climatic (air temperature and precipitation) and local (potential incident solar radiation, vegetation and soil properties) conditions at 30 arc-second spatial resolution were selected to examine their potential effects on MAGT and ALT at the circumpolar scale (e.g. Brown et al., 2000; French, 2007; Jorgenson et al., 2010; Bonnaventure & Lamoureux, 2013; Streletskiy et al., 2015). Climatic parameters were derived from the WorldClim dataset (Hijmans et al., 2005). The temporal coverage of WorldClim is 1950–2000, so we adjusted the data to match our study period of 2000–2014 using the Global Meteorological Forcing Dataset for land surface modelling (GMFD, Version 2, Sheffield et al., 2006) at a 0.5-degree resolution (see Aalto et al., 2018a). Monthly averages over this 15-year period were then used to derive the following climate parameters.

Previous studies have suggested that using indices representing the length or magnitude of thawing and freezing season could be more suitable than annual mean of air temperature (e.g. Zhang et al., 1997; Smith et al., 2009). Thus, thawing (TDD) and freezing (FDD) degree-days were determined as cumulative sums of mean monthly air temperatures above and below 0 °C, respectively. Frauenfeld et al. (2007) showed that their use instead of daily temperatures accounts for less than 5 % error for most high-latitude land areas. Since available global data on snow thickness or snow-water equivalency have relatively coarse spatial resolutions (Bokhorst et al., 2016), we examined the snow cover's contribution indirectly using derivatives of the climate data. We estimated annual snow and rainfall by summing up precipitation (mm) for months with mean monthly temperature below and above 0 °C, respectively (Zhang et al., 2003).

MODIS Terra-based normalized difference vegetation indices (NDVI, Didan, 2015) at a 1-km resolution were used to assess the amount of photosynthetic vegetation. We averaged monthly summertime (June to August) NDVI values over the study period of 2000–2014 and screened for only high-quality pixels based on the MODIS pixel reliability attribute. Potential incident solar radiation, computed after McCune and Keon (2002, Equation 2, p. 605) utilizing slope angle and aspect, along with latitude, was used to estimate the potential incident solar radiation (PISR, W cm^{-1} a^{-1}) that affects the energy balance of the ground thermal regime (e.g. Hasler et al., 2015; Streletskiy et al., 2015). Soil organic carbon content (SOC, g kg^{-1}), and fractions of coarse (CoarseSed, > 2 mm) and fine sediments (FineSed, ≤ 50 μm) for 0–200 cm subsurface, were extracted from SoilGrids database (Hengl et al., 2017).

2.3 Statistical modelling

2.3.1 Calibration of MAGT and ALT models

We used four statistical techniques, namely generalized linear modelling (GLM, McCullagh and Nelder, 1989), generalized additive modelling (GAM, Hastie and Tibshirani, 1990), and regression-tree based machine-learning methods generalized boosting method (GBM, Friedman et al., 2000) and random forest (RF, Breiman 2001) to calibrate MAGT and ALT models by using the nine geospatial predictors. Multi-model framework was adopted to control for uncertainties related to the choice of modeling algorithm (e.g. Marmion et al., 2009). GLM is an extension of linear regression capable of handling non-linear relationships with an adjustable link function between the response and explanatory variables. The GLM models were fitted including quadratic terms for each predictor. In GAM, alongside linear and polynomial terms, smoothing splines can be applied for more flexible handling of non-linear relationships. For smoothing spline, a maximum of three degrees of freedom were specified, which was further optimized by the model fitting function. To examine the direction and possible non-linearity of the relationship between predictors and responses, we used GAM to plot model-based response curves. The curves show smoothed fit between response and a predictor while all other predictors are fixed at their average (Hjort and Luoto, 2011). Both GLM and GAM were fitted without interactions between predictors using a Gaussian error distribution with an identity link function.

GBM was specified with the following parameters: number of trees = 3,000, interaction depth = 6, shrinkage = 0.001. Bagging fraction was set to 0.75 to select a random subset of 75 % of the observations at each step, without replacement. As for RF, 500 trees, each with a minimum node size of five were grown. The final prediction is the average of individual tree predictions. Both GBM and RF automatically consider interaction effects between predictors (Friedman et al., 2000). All statistical analyses were executed in R (R Core team, 2015) using auxiliary R packages; *mgcv* (Wood, 2011) for GAM, *dismo* (Hijmans et al., 2016) for GBM, and *randomForest* for RF (Liaw and Wiener, 2002).

2.3.2 Model evaluation

To evaluate the models, we split the response data randomly into calibration (70 % of the observations) and evaluation (30 %) datasets (Heikkinen et al., 2006). This was repeated 100 times, at each step fitting models with the calibration data and then using them to predict to both the calibration and evaluation datasets. Model performance was assessed with adjusted coefficient of determination (R^2) and root mean square error (RMSE) between observed and predicted values in these datasets.

2.3.3 Variable importance computation

A measure of variable importance was computed to determine the relative importance of each predictor to the models´ predictive performance (Breiman, 2001). In the computation, each modelling technique was first used to fit models with the MAGT and ALT datasets using all the nine predictors. The variable importance was then computed based on Pearson's correlation between predictions from two models produced with the fitted model; one with unchanged variables, and another where the values of one variable were randomized while others remained intact. In the procedure, each predictor was randomized in successive model runs. The measure of variable importance was computed as follows:

$$\text{Variable importance} = 1 - \text{corr}(\text{Prediction}_{\text{intact variables}}, \text{Prediction}_{\text{one variable randomized}}) \quad (1)$$

On a range from 0 to 1, high variable importance value, i.e. high individual contribution to MAGT or ALT, was returned when any randomized predictor had a substantial impact on the model's predictive performance, and consequently resulted low correlation with predictions from the model with intact variables (Thuiller et al., 2009). Each modelling method was run 100 times for each response with each predictor shuffled separately. For each run, different subsample from the original data was randomly bootstrapped with replacement.

2.3.4 Effect size statistics

Effect sizes for each predictor were determined based on the range between the predicted minimum and maximum MAGT and ALT values over the observation data while controlling for the influence of other predictors by fixing them at their mean values (see Nakagawa and Cuthill, 2007). The procedure was repeated with each dataset and modelling method.

3 Results

MAGT in permafrost conditions was on average –3.1 °C while the minimum was –15.5 °C. $MAGT_{>0\,°C}$ had an average of 8.0 °C and a maximum of 23.2 °C. ALT had an average of 141 cm and ranged from 23 to 733 cm. The extreme values, apart from the ALT maximum, were based on one year of measurements. Pairwise correlations and the scatter plots revealed a strong association between MAGT and air temperature, especially in $MAGT_{>0\,°C}$ (Fig. 2a–b, d). In contrast to MAGT, ALT was not significantly correlated with TDD, but had stronger associations with soil properties (Fig. 2c). Coarse sediments and SOC, especially, were important and showed clear, yet non-linear, responses to ALT, respectively (Fig. 4c). Statistical descriptives of the predictors in respective datasets are presented in Fig. S1.

3.1 Model performance

$MAGT_{>0\,°C}$ models had the highest R^2 values between predicted and observed MAGT (Table 1). In permafrost conditions, all the models had high R^2 values for MAGT, whereas in case of ALT between-model variation was large and R^2 on average lower. A decrease in the fit was identified when predicting ALT to evaluation datasets, especially with GBM and RF, whereas MAGT models retained their high performance. On average, RMSEs were low (~1 °C) in $MAGT_{\leq 0\,°C}$ and $MAGT_{>0\,°C}$ calibration datasets. When predicted over evaluation datasets, the average increased slightly more in non-permafrost conditions. A similar increase of 40 % was documented with ALT. For each response, GBM and RF had lower RMSEs (i.e. higher predictive performance) than GLM and GAM, but also larger change between calibration and evaluation datasets, indicating that GLM and GAM produced more robust predictions.

3.2 Relative importance of individual variables

FDD and TDD were the most important factors affecting MAGT; FDD (0.27) where permafrost was present, TDD (0.53) in non-permafrost conditions (Fig. 3a–b). Precipitation predictors, especially water precipitation, had a moderate importance (0.10) on $MAGT_{\leq 0\,°C}$ but were marginal when permafrost was not present (0.01). Climatic factors were followed by solar radiation (0.02, both MAGT datasets) and finally by NDVI and soil properties with minimal importance (each ≤0.01). The importance of both water and snow precipitation was higher in permafrost conditions.

Solar radiation was the most important predictor (0.37) explaining variation in ALT (Fig. 3c). Water precipitation had second highest importance (0.05) followed by soil properties SOC (0.04) and coarse sediments (0.03). The remaining climate variables (snow precipitation, TDD and FDD) had low importance scores that were comparable to those of NDVI (each 0.01–0.02).

3.3 Effect size of individual variables

FDD had the highest individual effect size of 6.7 °C averaged over the four methods in case of $MAGT_{\leq 0\,°C}$, whereas in $MAGT_{>0\,°C}$ dataset TDD accounted for a dominant 13.6 °C effect (Table 2). Precipitation had the second highest effect, albeit snow precipitation was less effective in non-permafrost conditions. Considering the remaining predictors, clear differences were observed in cases of SOC and NDVI, both higher in $MAGT_{>0\,°C}$ dataset. In case of ALT, water precipitation exerted the greatest effect (181 cm) despite large between-model variation. In contrast to variable importance results (Fig. 3c), snow precipitation had a larger average effect than coarse sediments and SOC, both of which nevertheless had a considerable effect. Solar radiation had a central role with a highly non-linear shape of response (Fig. 4c). A varying degree of non-linearity is also

visible in the responses between $MAGT_{\leq 0\ °C}$ and the key predictors, whereas in case of $MAGT_{>0\ °C}$ the responses are more linear (Fig. 4a–b).

4 Discussion

4.1 Circumpolar factors affecting MAGT and ALT

Our results are in line with previous understanding that climatic conditions are the primary factors affecting the long-term averages of circumpolar MAGT at 1-km resolution but also indicate that the effects of TDD and FDD on MAGT are dependent on the current permafrost occurrence. As anticipated, FDD has higher influence on MAGT in permafrost conditions where strong freezing is a prerequisite for the occurrence of permafrost (e.g. Smith & Riseborough, 1996). At sites without permafrost, TDD has the dominant nearly linear (Fig. 4b) effect, which is suggested to be mostly attributed to the lack of the buffering effect of the freeze-thaw processes and latent-heat exchange in the active layer (e.g. Osterkamp, 2007), and to the absence of seasonal snow cover in the warmest parts of the study region. In permafrost conditions, the warming effect of TDD and especially the cooling effect of FDD on MAGT show flattening in response shapes where MAGT is close to 0 °C owing to the latent-heat effects associated with thawing and freezing of water in the active layer (Fig. 4a).

The minimal effect of TDD on ALT contradicts with the documented strong regional scale (spatio)temporal connection (e.g. Zhang et al., 1997; Oelke et al., 2003; Frauenfeld et al., 2004; Melnikov et al., 2004; Yi et al., 2018). According to our results, the spatial linkage is more elusive at a broader scale and could be attributed to the great circumpolar variation in ALT. The majority of high-Arctic sites locate on low-lying tundra overlaid by mineral and organic soil layers, whereas at mid-latitudes (the Alps, central Asian mountain ranges) permafrost predominantly occurs in mountains with thin soils and thermally diffusive bedrock. This difference partly explains generally small and large ALT within the respective regions notwithstanding that they can have similar average climatic conditions (e.g. TDD, see Fig. 2d). Moreover, large inconsistencies between observed ALT and climate-warming trends have been documented (e.g. Wu et al., 2012; Gangodagamage et al., 2014). Although temporal dynamics of ALT are beyond our analyses, this suggests that thaw depth and air temperatures are, to a degree, decoupled by local conditions.

Recent warming trends in the atmosphere (Guo et al., 2017) are already well visible in circumpolar permafrost temperature observations (Romanovsky et al., 2017) implying that the permafrost system will remain dynamic in future's changing climate. Warmer air temperatures will occur mostly during winters (AMAP, 2017; Guo et al., 2017), which, given the presented high contribution of FDD on MAGT, suggests that changes are foreseeable. Projected warmer winters can also affect ALT through changing snow conditions and subsequent changes in hydrology and vegetation (Park et al., 2013; Atchley et al., 2016; Peng et al., 2018).

In line with new studies (Peng et al., 2018; Zhang et al., 2018), our results highlight the notable role of water precipitation on both MAGT and ALT. Projected greater proportion of liquid precipitation (e.g. AMAP, 2017; Bintanja and Andry, 2017) potentially has a direct effect on the ground thermal regime through its influence on latent heat exchange (Westermann et al., 2011), and convective warming during spring (Kane et al., 2001) and summertime (Melnikov et al., 2004; Marmy et al., 2013). However, abundant summer rains arguably also cool the ground surface through increased evaporation and heat capacity, and thus limit the heat conduction into the ground (Zhang et al., 1997, 2005; Frauenfeld et al., 2004; Park et al., 2013). Moreover, extreme climatic events, such as wintertime rain events can have a distinct effect on soil temperature (Westermann et al., 2011) although the long-term sensitivity of permafrost to them is not fully clear yet (Marmy et al., 2013). According to Kurylyk et al. (2014), permafrost studies often consider only conductive heat propagation in the ground. Vincent et al. (2017), however, stress the need to acknowledge processes associated with liquid water and advective heat in efforts to understand rapidly changing cryosphere.

The dominant contribution of water precipitation over snowfall observed here contradicts with some previous regional scale studies (e.g., Zhang et al., 2003, 2005). However, the elevated effect of snowfall on MAGT in permafrost conditions (effect size of 2.3 °C compared to 0.8 °C in non-permafrost conditions) underlines the role of snow cover's control over the ground thermal regime. Similarly, Zhang et al. (2018) found that the offset between air and surface temperatures was weaker in temperate regions (mean annual air temperature >0 °C) than in low-Arctic and boreal permafrost regions, although also high-Arctic had small offsets owing to small amount of snow. Despite the complexity involved in the role of snow conditions (e.g. Fiddes et al., 2015; Aalto et al., 2018b), thick snow cover has been shown to increase also ALT at site (Atchley et al., 2016), regional (Zhang et al., 1997; Frauenfeld et al., 2004) and circumpolar scale (Park et al., 2013).

Incoming solar energy can be considered central for soil thawing (see Biskaborn et al., 2015), but the high contribution of solar radiation on ALT stands out. Arguably, the effect is emphasized because ALT observation sites in cold permafrost conditions are mostly sparse in vegetation and lack tree canopy (Zhang et al., 2003; Biskaborn et al., 2015). Moreover, most of the ALT sites have been established on flat terrain (Biskaborn et al., 2015), meaning that local topographic shading is less significant. Thus, ALT is suggested to follow poleward decrease in solar radiation and associated shorter thaw seasons (see Luo et al., 2016). The weaker association of solar radiation with MAGT suggests that its direct effect is limited to the near-surface permafrost, i.e. intensified thawing during thawing seasons, and that the influence to deeper temperatures is more indirect and associated with the relationship between annual solar radiation and air temperatures. Moreover, given that MAGT sites are usually located in more topographically heterogeneous terrain than ALT sites, the local exposure to solar radiation is suggested to be more important than the latitudinal trend (e.g. Romanovsky et al. 2010).

The weak connection between TDD and ALT is additionally explained by soil factors that influence the heat transfer between the lower atmosphere and the ground (Smith et al., 2009). According to the response shapes from GAM, coarse sediments increase ALT when enough prevalent (~25 % fraction) in the soils. The effect of soil texture on ALT has been implied to occur largely through its effects on hydrological conditions (Zhang et al., 2003; Yin et al., 2017) and conductivity (Callaghan et al., 2011). More efficient water transfer in coarse-grained material could impose convective heat into soils during the thawing season or promote latent-heat effect during the freeze-up, which both contribute to deeper thaw (see Romanovsky and Osterkamp, 2000; Frauenfeld et al., 2004). Insulation by soil organic layers has been demonstrated to effectively decouple air-permafrost connection resulting in thinner active layer and lower soil temperatures (e.g. Johnson et al., 2013; Atchley et al., 2016). The GAM response shape illustrates a thinning of ALT with increasing SOC until ~150 g kg^{-1}, after which additional organic material does not attribute to enhanced insulation.

NDVI has a small contribution on ALT and MAGT in permafrost conditions, but outside the permafrost region it has a moderate cooling effect. The low contribution of NDVI in permafrost conditions could be attributed to the intra- and inter-seasonal differences in the effects of vegetation. In wintertime, low vegetation traps snow and thereby enhances insulation of the ground. Taller tree canopies of evergreen boreal forests, in turn, intercept snow and allow more heat loss from the ground in winter, while in summer their shading cools the ground surface (Lawrence and Swenson, 2011; Fisher et al., 2016).

4.2 Uncertainties

Large-scale scrutinization of factors affecting ground thermal dynamics is often hindered by data deficiencies or unavailability. More precisely, many data lack adequate spatial or temporal accuracy, geographical consistency, methodological robustness or thematic detail (Bartsch et al., 2016; Chadburn et al., 2017). Some of these shortcomings are exacerbated in remote permafrost regions with low-density observational networks of, e.g., climatic parameters (Hijmans et al., 2005) or soil profiles (Hengl et al., 2017). The fine-scale spatial variability of ALT and MAGT called for a high spatial resolution data to assess the local factors that mediate the atmospheric forcing. Here, the availability of geospatial data largely determined the resolution of 30 arc seconds, which could be considered the highest currently attainable resolution at a near-global scale. While not

adequate to account for all potential sources of sub-grid spatial heterogeneity in, e.g. microclimatic conditions, especially in topographically complex conditions (Fiddes et al., 2015; Aalto et al., 2018b; Yi et al., 2018), the implemented resolution is a step forward in making a distinction in between-site conditions and revealing local relationships relevant at the circumpolar scale.

In general, the sensitivity of MAGT to the climatic parameters along with the minimal role of soil and vegetation properties suggests that circumpolar future predictions of MAGT are more applicable than those of ALT, even without addressing, for example, future vegetation or soil organic carbon content, whose response to climate change is extremely challenging to project (Jorgenson et al., 2013). However, the effects of soil properties on MAGT have been shown to be statistically significant when predicting future circumpolar ground thermal conditions (Aalto et al., 2018a), and should thus be considered. In addition, Throop et al. (2012), for example, concluded that substrate greatly affects the spatial distribution of permafrost, and that bedrock is expected to respond more rapidly to changes in climate than unconsolidated sediments. Given the pronounced role of precipitation, more direct information on fine-scale soil moisture conditions controlled by local soil and land surface properties (see Kemppinen et al., 2018), as well as more comprehensive and finer resolution data on circumpolar snow thickness are required for improved ground thermal regime modelling. Fine-scale biophysical factors affecting drainage conditions and distribution of wind-drifted snow (e.g. vegetation and small topo-graphic depressions) are largely averaged-out and cannot be accounted for at 1-km resolution.

Although the main factors were identified as important and effective by each modelling technique, notable inter-modal variability suggested that using only one method could have led to disputable results. A multi-model approach was in this sense safer, although not all the methods may have worked optimally with the present observational and environmental data owing to their different abilities to handle collinearity, spatial autocorrelation or non-linearity. For example, interactions between variables were not included in regression-based modelling (GLM and GAM), while being intrinsically considered by tree-based methods (GBM and RF) (Friedman et al., 2000). Differences such as this could have attributed to the dissimilar performances of the models; GBM and RF were overall less stable when comparing R^2 and RMSE values between the observed and predicted values in calibration and evaluation settings.

5 Conclusions

We assessed the factors affecting the circumpolar ground thermal regime at an unprecedentedly high 1-km spatial resolution using comprehensive field-quantified observational datasets on MAGT and ALT. Our statistical modelling framework efficiently captured the multi-variate nature of ground thermal regime and highlighted the difference between the contributions of climatic factors on MAGT inside and outside the permafrost domain. In permafrost conditions, different key factors accounted for variation in MAGT and ALT; climate was paramount for MAGT, while local environmental conditions were emphasized in case of ALT. Our 1-km scale findings are congruent with previous process- and broad-scale studies stressing that, in addition to reliably addressing the key climatic factors, realistic modelling of Earth surface systems should take into account local-scale variation in solar radiation and ground properties. In addition to providing theoretical insights about effective magnitudes and directions of the key contributing factors at circumpolar scale, multi-variate modelling frameworks capable of employing high-resolution geospatial data are valuable for the spatio-temporal prediction of ground thermal regime at circumpolar scale.

Author contribution

OK, ML and JH developed the original idea. OK led the compilation of observational data and geospatial data processing with contributions from all the authors. ML, OK and JA performed the statistical analyses. OK wrote the manuscript with contributions from all the authors.

Acknowledgements. This study was funded by the Academy of Finland (grants 285040 and 286950).

Competing interests

The authors declare that they have no conflict of interest.

References

Aalto, J., Harrison, S., and Luoto, M.: Statistical modelling predicts almost complete loss of major periglacial processes in Northern Europe by 2100, Nat. Commun., 8, doi.org/10.1038/s41467-017-00669-3, 2017.

Aalto, J., Karjalainen, O., Hjort, J., and Luoto, M.: Statistical Forecasting of Current and Future Circum-Arctic Ground Temperatures and Active Layer Thickness, Geophys. Res. Lett., 45, doi.org/10.1029/2018GL078007, 2018a.

Aalto, J., Scherrer, D., Lenoir, J., Guisan, A., and Luoto, M.: Biogeophysical controls on soil-atmosphere thermal differences: implications on warming Arctic ecosystems, Environ. Res. Lett., 13, doi.org/10.1088/1748-9326/aac83e, 2018b.

AMAP: Snow, Water, Ice and Permafrost in the Arctic (SWIPA): Climate Change and the Cryosphere, Arctic Monitoring and Assessment Programme (AMAP), Oslo, Norway, 2017.

Atchley, A. L., Coon, E. T., Painter, S. L., Harp, D. R., and Wilson, C. J.: Influences and interactions of inundation, peat, and snow on active layer thickness, Geophys. Res. Lett., 43, 5116–5123, doi:10.1002/2016GL068550, 2016.

Bartsch, A., Höfler, A., Kroisleitner, C., and Trofaier, A. M.: Land cover mapping in northern high latitude permafrost regions with satellite data: achievements and remaining challenges, Remote Sens., 8, 979, doi:10.3390/rs8120979, 2016.

Bintanja, R. and Andry, O.: Towards a rain-dominated Arctic. Nat. Clim. Change, 7, 263–267, doi: 10.1038/nclimate3240, 2017.

Biskaborn, B. K., Lanckman, J.–P., Lantuit, H., Elger, K., Streletskiy, D. A., Cable, W. L., and Romanovsky, V. E.: The new database of the Global Terrestrial Network for Permafrost (GTN-P), Earth Syst. Sci. Data 7, 245–259, 2015.

Bokhorst, S., Højlund Pedersen, S., Brucker, L., Anisimov, O., Bjerke, J. W., Brown, R. D., Ehrich, D., Essery, R. L. H., Heilig, A., Ingvander, S., Johansson C., Johansson, M., Jónsdóttir, I. S., Inga, N., Luojus, K., Macelloni, G., Mariash, H., McLennan, D., Rosqvist, G. N., Sato, A., Savela, H., Schneebeli, M., Sokolov, A., Sokratov, S. A., Terzago, S., Vikhamar-Schuler, D.,Williamson, S., Qiu, Y., and Callaghan, T. V.: Changing Arctic snow cover: A review of recent developments and assessment of future needs for observations, modelling, and impacts, Ambio, 45, doi:10.1007/s13280-016-0770-0, 2016.

Bonnaventure, P. P. and Lamoureux, S. F.: The active layer: A conceptual review of monitoring, modelling techniques and changes in a warming climate, Prog. Phys. Geog., 37, 352–376, 2013.

Breiman, L.: Random forests, Machine Learning 45, 5–32, 2001.

Brown, J., Hinkel, K. M., and Nelson, F. E.: The circumpolar active layer monitoring (CALM) program: research designs and initial results, Polar Geography, 24, 165–258, 2000.

Brown, J., Ferrians, O. J. Jr., Heginbottom, J. A., and Melnikov, E. S.: Circum-Arctic Map of Permafrost and Ground-Ice Conditions,Version 2, National Snow and Ice Data Center, http://nsidc.org/data/ggd318, 2002.

Callaghan, T. V., Johansson, M., Anisimov, O., Christiansen, H. H., Instanes, A., Romanovsky, V. E., and Smith, S.: Changing permafrost and its impacts, in: Snow, Water, Ice and Permafrost in the Arctic (SWIPA): Climate Change and the Cryosphere, Arctic Monitoring and Assessment Programme (AMAP), Oslo, Norway, 2011.

Chadburn, S. E.,Burke, E. J., Cox, P. M., Friedlingstein, P., Hugelius, G., and Westermann, S.: An observation-based constraint on permafrost loss as a function of global warming, Nat. Clim. Change, 7, doi:10.1038/nclimate3262, 2017.

Didan, K.: MOD13A2 MODIS/Terra Vegetation Indices 16-Day L3 Global 1km SIN Grid V006. NASA EOSDIS LP DAAC. doi: 10.5067/MODIS/MOD13A2.006, 2015.

Ekici, A., Chadburn, S., Chaudhary, N., Hajdu, L. H., Marmy, A., Peng, S., Boike, J., Burke, E., Friend, A. D., Hauck, C., Krinner, G., Langer, M., Miller, P. A., and Beer, C.: Site-level model intercomparison of high latitude and high altitude soil thermal dynamics in tundra and barren landscapes, The Cryosphere, 9, 1343–1361, 2015.

Etzelmüller, B.: Recent advances in mountain permafrost research, Permafrost Periglac., 24, 99–107, 2013.

Etzelmüller, B., Schuler, T. V., Isaksen, K., Christiansen, H. H., Farbrot, H., and Benestad, R.: Modeling the temperature evolution of Svalbard permafrost during the 20th and 21st century, The Cryosphere, 5, 67–79, 2011.

Fiddes, J., Endrizzi, S., and Gruber, S.: Large-area land surface simulations in heterogeneous terrain driven by global data sets: application to mountain permafrost, The Cryosphere, 9, 411–426, 2015.

Fisher, J. P., Estop-Aragonés, C., Thierry, A., Charman, D. J., Wolfe, S. A., Hartley, I. P., Murton, J. B., Williams, M., and Phoenix, G. K.: The influence of vegetation and soil characteristics on active-layer thickness of permafrost soils in boreal forest, Glob. Change Biol., 22, 3217–3140, 2016.

Frauenfeld, O. W., Zhang, T., and Barry, R. G.: Interdecadal changes in seasonal freeze and thaw depths in Russia, J. Geophys. Res., VOL. 109, D05101, doi:10.1029/2003JD004245, 2004.

Frauenfeld, O. W., Zhang, T. and McCreight J. L.: Northern hemisphere freezing/thawing index variations over the twentieth century, Int. J. Climatol., 27, 47–63, 2007.

French, H. M.: The Periglacial Environment, 3rd Edn, Wiley, 2007.

Friedman, J., Hastie, T., and Tibshirani, R.: Additive logistic regression: a statistical view of boosting, The Annals of Statistics, 28, 337–407, 2000.

Gangodamage, C., Rowland, J. C., Hubbard, S. S., Brumby, S. P., Liljedahl, A. K., Wainwright, H., Wilson, C. J., Altmann, G. L., Dafflon, B., Peterson, J., Ulrich, C., Tweedie, C. E., and Wullschleger, S. D.: Extrapolating active layer thickness measurements across Arctic polygonal terrain using LiDAR and NDVI data sets, Water Resour. Res., 50, 6339–6357, doi:10.1002/2013WR014283, 2014.

Grosse, G., Goetz, S., McGuire, A. D., Romanovsky, V. E. and Schuur, E. A. G.: Changing permafrost in a warming world and feedbacks to the Earth system, Environ. Res. Lett., 11, 2016.

Gruber, S., Fleiner, R., Guegan, E., Panday, P., Schmid, M.-O., Stumm, D., Wester, P., Zhang, Y., and Zhao, L.: Review article: Inferring permafrost and permafrost thaw in the mountains of the Hindu Kush Himalaya region, The Cryosphere 11, 81–99, 2017.

Guo, D., Li, D., and Hua, W.: Quantifying air temperature evolution in the permafrost region from 1901 to 2014, Int. J. Climatol., 38, 66–76, doi: 10.1002/joc.5161, 2017.

Harlan, R. L. and Nixon J. F.: Ground thermal regime, in: Geotechnical Engineering for Cold Regions, Andersland, O.B. and Anderson, D.M. (Eds.), McGraw-Hill, New York, 103–163, 1978.Hasler, A., Geertsema, M., Foord, V., Gruber, S., and Noetzli, J.: The influence of surface characteristics, topography and continentality on mountain permafrost in British Columbia, The Cryosphere, 9, 1025–1038, 2015.

Hastie, T. J. and Tibshirani, R. J.: Generalized Additive Models, CRC Press, 1990.

Heikkinen, R. K., Luoto, M., Araújo, M. B., Virkkala, R., Thuiller, W., and Sykes, M. T.: Methods and uncertainties in bioclimatic envelope modelling under climate change, Prog. Phys. Geog., 30, 751–777, 2006.

Hengl, T., Mendes de Jesus, J., Heuvelink, G.B.M., Ruiperez Gonzalez, M., Kilibarda, M., Blagotić, A., Shangguan, W., Wright, M. N., Geng, X., Bauer-Marschallinger, B., Antonio Guevara, M., Vargas, R., MacMillan, R. A., Batjes, N. H., Leenaars, J. G. B., Ribeiro, E., Wheeler, I., Mantel, S., and Kempen, B.: SoilGrids250m – Global gridded soil information based on machine learning, PLoS ONE 12, e0169748, doi.org/10.1371/journal.pone.0169748, 2017.

Hijmans, R. J., Cameron, S. E., Parra, J. L., Jones, P. G., and Jarvis, A.: Very high resolution interpolated climate surfaces for global land areas, Int. J Climatol., 25, 1965–1978, 2005.

Hijmans, R. J., Phillips S., Leathwick, J., and Elith, J.: dismo: Species Distribution Modeling. R package version 1.1-1. http://cran.r-project.org/web/packages/dismo/index.html, 2016.

Hjort, J. and Luoto, M.: Novel theoretical insights into geomorphic process–environment relationships using simulated response curves, Earth Surf. Process. Landforms, 36, 363–371, 2011.

Johnson, K. D., Harden, J. W., McGuire, A. D., Clark, M., Yuan, F., and Finley, A. O.: Permafrost and organic layer interactions over a climate gradient in a discontinuous permafrost zone, Environ. Res. Lett., 8, 035028, 2013.

Jorgenson, M. T., Romanovsky, V., Harden, J., Shur, Y., O'Donnell, J., Schuur, E. A. G., Kanevskiy, M., and Marchenko, S.: Resilience and vulnerability of permafrost to climate change, Can. J. For. Res., 40, 1219–1236, 2010.

Jorgenson, M. T., Harden, J., Kanevskiy, M., O'Donnell, J., Wickland, K., Ewing, S., Manies, K., Zhuang, Q., Shur, Y., Striegl, R., and Koch, J.: Reorganization of vegetation, hydrology and soil carbon after permafrost degradation across heterogeneous boreal landscapes, Environ. Res. Lett., 8, 035017, 2013.

Kane, D. L., Hinkel, K. M., Goering, D. J., Hinzman, L. D., and Outcalt, S. I.: Non-conductive heat transfer associated with frozen soils, Glob. Planet. Change, 29, 275–292, 2001.

Kemppinen, J., Niittynen, P., Riihimäki, H., and Luoto, M.: Modelling soil moisture in a high-latitude landscape using LiDAR and soil data, Earth Surf. Process. Landforms, 43, 1019–1031, doi: 10.1002/esp.4301, 2018.

Kurylyk, B. L., MacQuarrie, K. T. B., and McKenzie, J. M.: Climate change impacts on groundwater and soil temperatures in cold and temperature regions: Implications, mathematical theory, and emerging simulation tools, Earth-Sci. Rev., 138, 313–334, 2014.

Lawrence, D. M. and Swenson, S. C.: Permafrost response to increasing Arctic shrub abundance depends on the relative influence of shrubs on local soil cooling versus large-scale climate warming, Environ. Res. Lett., 6, 045504, 2011.

Liaw, A. and Wiener, M.: Classification and regression by randomForest, R news 2, 18–22, 2002.

Liljedahl, A. K., Boike J., Daanen, R. P., Fedorov, A. N., Frost, G. V.,Grosse, G., Hinzman, L. D., Iijma, Y., Jorgenson, J. C., Matveyeva, N., Necsoiu, M., Raynolds, M. K., Romanovsky, V. E., Schulla, J., Tape, K. D., Walker, D. A., Wilson, C. J., Yabuki, H., and Zona, D.: Pan-Arctic ice-wedge degradation in warming permafrost and its influence on tundra hydrology, Nat. Geosci., 9, doi: 10.1038/ngeo2674, 2016.

Luo, D., Wu, Q., Jin, H., Marchenko, S. S., Lü, L., and Gao, S.: Recent changes in the active layer thickness across the northern hemisphere, Environ. Earth Sci., 75:555, doi:10.1007/s12665-015-5229-2, 2016.

Marmion, M., Parviainen, M., Luoto, M., Heikkinen, R. K., and Thuiller, W.: Evaluation of consensus methods in predictive species distribution modelling, Divers. Distrib., 15, 59–69, 2009.

Marmy, A., Salzmann, N., Scherler, M., and Hauck, C.: Permafrost model sensitivity to seasonal climatic changes and extreme events in mountainous regions, Env. Res. Lett., 8, 035048, 2013.

McCullagh, P. and Nelder, J.: Generalized Linear Models, 2nd edn, Chapman-Hall, London, 1989.

McCune, B. and Keon, D.: Equations for potential annual direct incident radiation and heat load, J. Veg. Sci., 13, 603–606, 2002.

Melnikov, E. S., Leibman, M. O., Moskalenko, N. G., and Vasiliev, A. A.: Active-layer monitoring in the cryolithozone of West Siberia, Polar Geography, 28, 267–285, 2004.

Nakagawa, S. & Cuthill, I. C.: Effect size, confidence interval and statistical significance: a practical guide for biologists, Biol. Rev., 82, 591–605, 2007.

Oelke, C., Zhang, T., Serreze, M. C., and Armstrong, R. L.: Regional-scale modeling of soil freeze/thaw over the Arctic drainage basin, J. Geophys. Res., 108, D10, 4314, doi:10.1029/2002JD002722, 2003.

Osterkamp, T. E.: Characteristics of the recent warming of permafrost in Alaska, J. Geophys. Res., 112, F02S02, doi:10.1029/2006JF000578, 2007.

Park, H., Walsh, J., Fedorov, A. N., Sherstiukov, A. B., Iijima, Y., and Ohata, T.: The influence of climate and hydrological variables on opposite anomaly in active-layer thickness between Eurasian and North American watersheds, The Cryosphere, 7, 631–645, 2013.

Peng, X., Zhang, T., Frauenfeld, O. W., Wang, K., Luo, D., Cao, B., Su, H., Jun, H., and Wu, Q.: Spatiotemporal changes in active layer thickness under contemporary and projected climate in the Northern Hemisphere, J. Clim., 31, 251–266, 2018.

R Core Team: R: A language and environment for statistical computing. R Foundation for Statistical Computing, Vienna, Austria, https://www.r-project.org/, 2015.

Romanovsky, V. E. and Osterkamp, T. E.: Effects of unfrozen water on heat and mass transport processes in the active layer and permafrost, Permafrost Periglac., 11, 219–239, 2000.

Romanovsky, V. E., Smith, S. L. and Christiansen, H. H.: Permafrost thermal state in the polar northern hemisphere during the International Polar Year 2007–2009: a synthesis, Permafrost Periglac., 21, 106–116, 2010.

Romanovsky, V.E., Smith, S.L., Shiklomanov, N.I., Streletskiy, D.A., Isaksen, K., Kholodov, A.L., Christiansen, H.H., Drozdov, D.S., Malkova, G.V. and Marchenko, S.S.: Terrestrial Permafrost, Bulletin of the American Meteorological Society, 98, 147–149, 2017.

Sheffield, J., Goteti, G., and Wood, E. F.: Development of a 50-year high-resolution global dataset of meteorological forcings for land surface modeling, J. Clim., 19, 3088–3111, 2006.

Shiklomanov, N. I.: Non-climatic factors and long-term, continental-scale changes in seasonally frozen ground. Environ. Res. Lett., 7, 011003, doi:10.1088/1748-9326/7/1/011003, 2012.

Smith, M. W. and Riseborough, D. W.: Permafrost monitoring and detection of climate change, Permafrost and Periglac., 7, 301–309, 1996.

Smith, S. L., Wolfe, S. A., Riseborough, D. W., and Nixon, M.: Active-layer characteristics and summer climate indices, Mackenzie Valley, Northwest Territories, Canada, Permafrost Periglac., 20, 201–220, 2009.

Streletskiy, D. A., Anisimov, O., and Vasiliev, A.: Permafrost degradation, in: Snow and ice-related hazards, risks and disasters, Haeberli, W. and Whiteman, C. (Eds.), Elsevier, 303–344, 2015.

Throop, J., Lewkowicz, A. G., and Smith, S. L.: Climate and ground temperature relations at sites across the continuous and discontinuous permafrost zones, northern Canada, Can. J. Earth Sci., 49, 865–876, 2012.

Thuiller, W., Lafourcade, B., Engler, R., and Araújo, M. B.: BIOMOD – a platform for ensemble forecasting of species distribution, Ecography, 32, 369–373, 2009.

Vincent, W. F., Lemay, M., and Allard, M.: Arctic permafrost landscapes in transition: towards integrated Earth system approach, Arctic Science 3, 39–64, 2017.

Westermann, S., Boike, J., Langer, M., Schuler, T. V., and Etzelmüller, B.: Modeling the impact of wintertime rain events on the thermal regime of permafrost, The Cryosphere, 5, 945–959, 2011.

Westermann, S., Duguay, C. R., Grosse, G., and Kääb, A.: Remote sensing of permafrost and frozen ground, in: Remote Sensing of the Cryosphere, Tedesco, M. (ed.), Wiley, 307–344, 2015.

Woo, M.: Permafrost Hydrology, Springer-Verlag, Berlin Heidelberg, 2012.

Wood, S. N.: Fast stable restricted maximum likelihood and marginal likelihood estimation of semiparametric generalized linear models, J. R. Statist. Soc. B (Statistical Methodology), 73, 3–36, 2011.

Wu, Q., Zhang, T., and Liu, Y.: Thermal state of the active layer and permafrost along the Qinghai-Xizang (Tibet) Railway from 2006 to 2010, The Cryosphere, 6, 607–612, 2012.

Zhang, T., Osterkamp, T. E., and Stamnes, K.: Effects of climate on the active layer and permafrost on the North Slope of Alaska, U.S.A., Permafrost Periglac., 8, 45–67, 1997.

Zhang, T., Chen, W., Smith, S. L., Riseborough, D. W., and Cihlar, J.: Soil temperature in Canada during the twentieth century: complex responses to atmospheric climate change, J. Geophys. Res, 110, D03112, doi:10.1029/2004JD004910, 2005.

Zhang, Y., Chen, W., and Cihlar, J.: A process-based model for quantifying the impact of climate change on permafrost thermal regimes, J. Geophys. Res., 108, D22, 4695, doi:10.1029/2002JD003354, 2003.

Zhang, Y., Sherstiukov, A. B., Qian, B., Kokelj, S. V., & Lantz, T. C.: Impacts of snow on soil temperature observed across the circumpolar north, Environ. Res. Lett., 13, 044012, doi.org/10.1088/1748-9326/aab1e7, 2018.

Yi, Y., Kimball, J. S., Chen, R. H., Moghaddam, M., Reichle, R. H., Mishra, U., Zona, D., and Oechel, W. C.: Characterizing permafrost active layer dynamics and sensitivity to landscape spatial heterogeneity in Alaska, The Cryosphere, 12, 145–161, 2018.

Yin, G., Niu, F., Lin, Z., Luo, J., and Liu, M.: Effects of local factors and climate on permafrost conditions and distribution in Beiluhe basin, Qinghai-Tibet Plateau, China, Sci. Total Environ., 581-582, 472–485, 2017.

Table 1: Adjusted coefficient of determination (R^2) and root mean square error (RMSE) between observed and predicted mean annual ground temperature (MAGT) and active-layer thickness (ALT) in calibration and evaluation (in brackets) datasets averaged over 100 permutations. GLM = generalized linear modelling, GAM = generalized additive modelling, GBM = generalized boosting method and RF = random forest.

	$MAGT_{\leq 0\,°C}$		$MAGT_{>0\,°C}$		ALT	
Method	R^2	RMSE (°C)	R^2	RMSE (°C)	R^2	RMSE (cm)
GLM	0.86 (0.83)	1.24 (1.33)	0.95 (0.92)	1.20 (1.44)	0.65 (0.50)	80 (93)
GAM	0.88 (0.84)	1.17 (1.29)	0.95 (0.92)	1.18 (1.37)	0.70 (0.54)	74 (89)
GBM	0.93 (0.86)	0.88 (1.22)	0.97 (0.92)	0.91 (1.37)	0.84 (0.59)	55 (84)
RF	0.98 (0.87)	0.51 (1.17)	0.99 (0.93)	0.55 (1.27)	0.93 (0.62)	36 (82)
Average	0.91 (0.85)	0.95 (1.25)	0.96 (0.92)	0.96 (1.36)	0.78 (0.56)	61 (87)

Table 2: The effect size of individual predictors and their four-model averages (see Sect. 2.2 for abbreviations) in the original scale of the responses, °C for (mean annual ground temperature) MAGT and cm for active-layer thickness (ALT). The values are shaded with increasing blue ($MAGT_{\leq 0\,°C}$), red ($MAGT_{>0\,°C}$) and yellow (ALT) hues relative to the magnitude of the effect. GLM = generalized linear modelling, GAM = generalized additive modelling, GBM = generalized boosting method and RF = random forest. See Sect. 2.2 for predictor abbreviations.

	MAGT≤ 0°C (°C)					**MAGT> 0°C (°C)**					**ALT (cm)**				
	GLM	GAM	GBM	RF	Avg	GLM	GAM	GBM	RF	Avg	GLM	GAM	GBM	RF	Avg
FDD	8.6	10.7	4.3	3.2	6.7	3.8	4.3	2.6	2.8	3.4	117	86	15	36	64
TDD	7.1	6.6	2.4	2.8	4.7	19.1	19.5	9.0	6.6	13.6	30	23	19	31	26
PrecipWater	1.6	2.6	4.3	3.0	2.9	4.8	3.6	0.2	0.7	2.3	372	249	28	74	181
PrecipSnow	4.4	4.4	0.1	0.2	2.3	0.8	1.4	0.3	0.5	0.8	195	146	44	94	120
SolarRad	2.6	2.5	0.2	0.3	1.4	2.0	2.3	0.9	1.6	1.7	135	193	178	139	161
CoarseSed	0.8	1.8	0.1	0.2	0.7	0.6	2.6	0.1	0.3	0.9	129	137	69	65	100
FineSed	0.5	0.7	0.2	0.4	0.4	0.6	0.7	0.1	0.1	0.4	17	20	7	9	13
SOC	0.5	0.4	0.3	0.8	0.5	1.7	1.4	0.1	0.6	0.9	121	129	30	28	77
NDVI	0.4	0.3	0.1	0.8	0.4	2.6	2.3	0.2	0.1	1.3	68	36	15	34	38

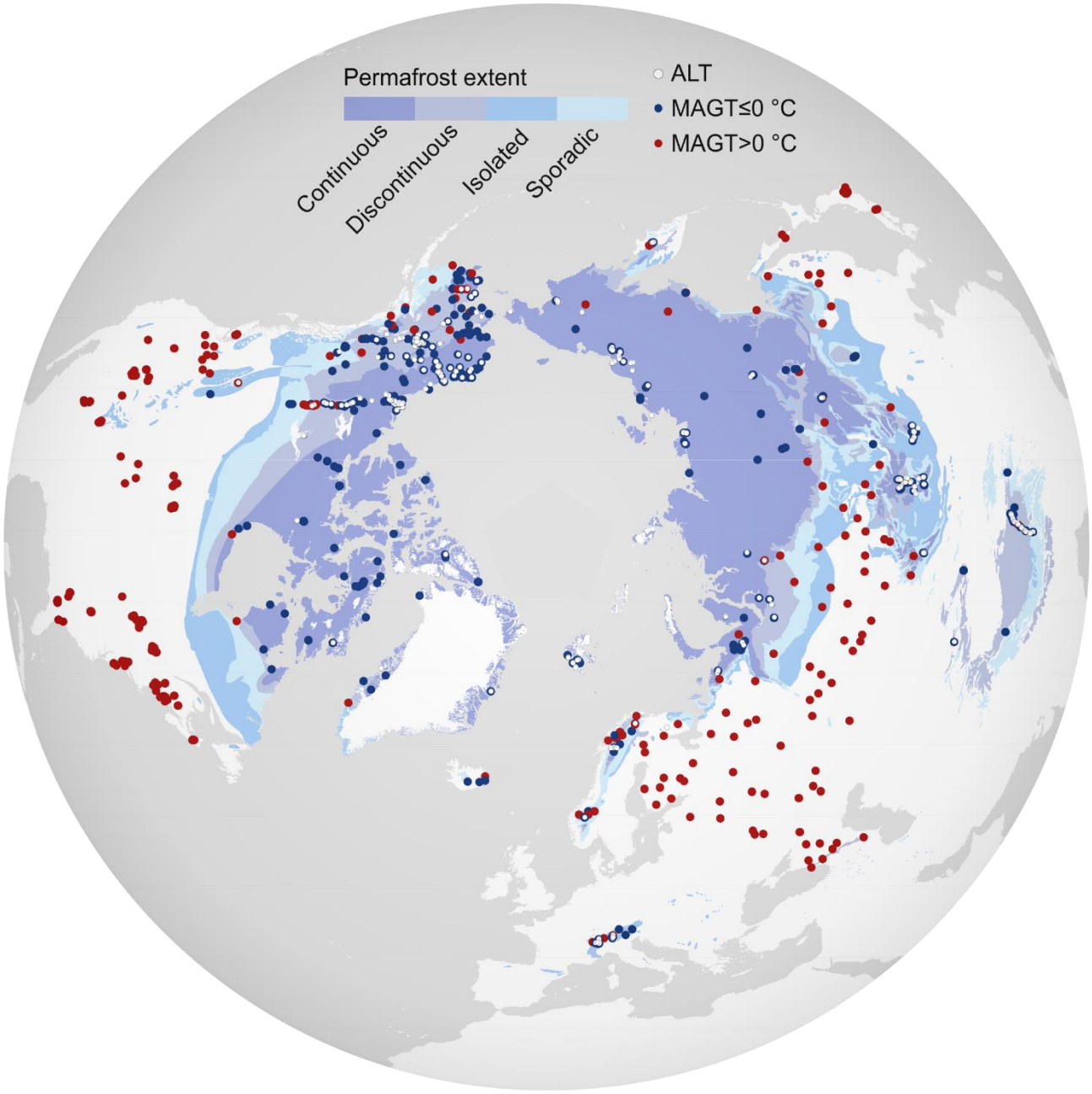

Figure 1: The observational network of the used mean annual ground temperature (MAGT) and active-layer thickness (ALT) across the circumpolar region. Blue symbols indicate the locations of boreholes where MAGT (averaged over the period 2000–2014) was at or below 0 °C and red symbols for those above 0 °C. White symbols depict the ALT measurements sites. The underlying permafrost zonation is from Brown et al. (2002).

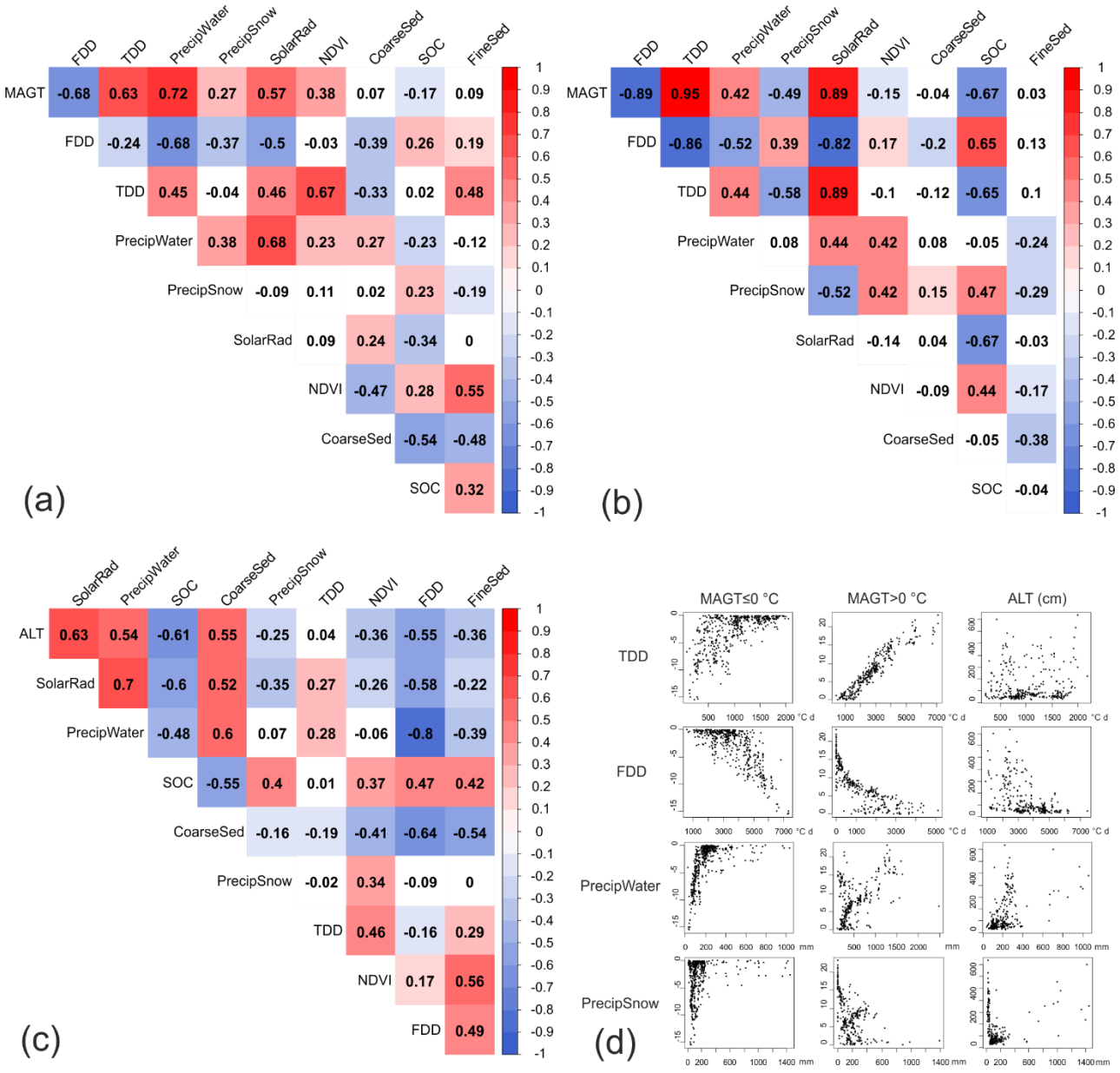

Figure 2: Spearman rank-order correlations between the predictor variables (see Sect. 2.2 for abbreviations) and $MAGT_{\leq 0\,°C}$ (mean annual ground temperature) (a), $MAGT_{>0\,°C}$ (b) and ALT (active-layer thickness) (c). Red hue stands for positive correlations, blue for negative, and white indicates non-significant ($p > 0.01$) correlations. Panel (d) shows MAGT and ALT observations plotted against the climatic predictors.

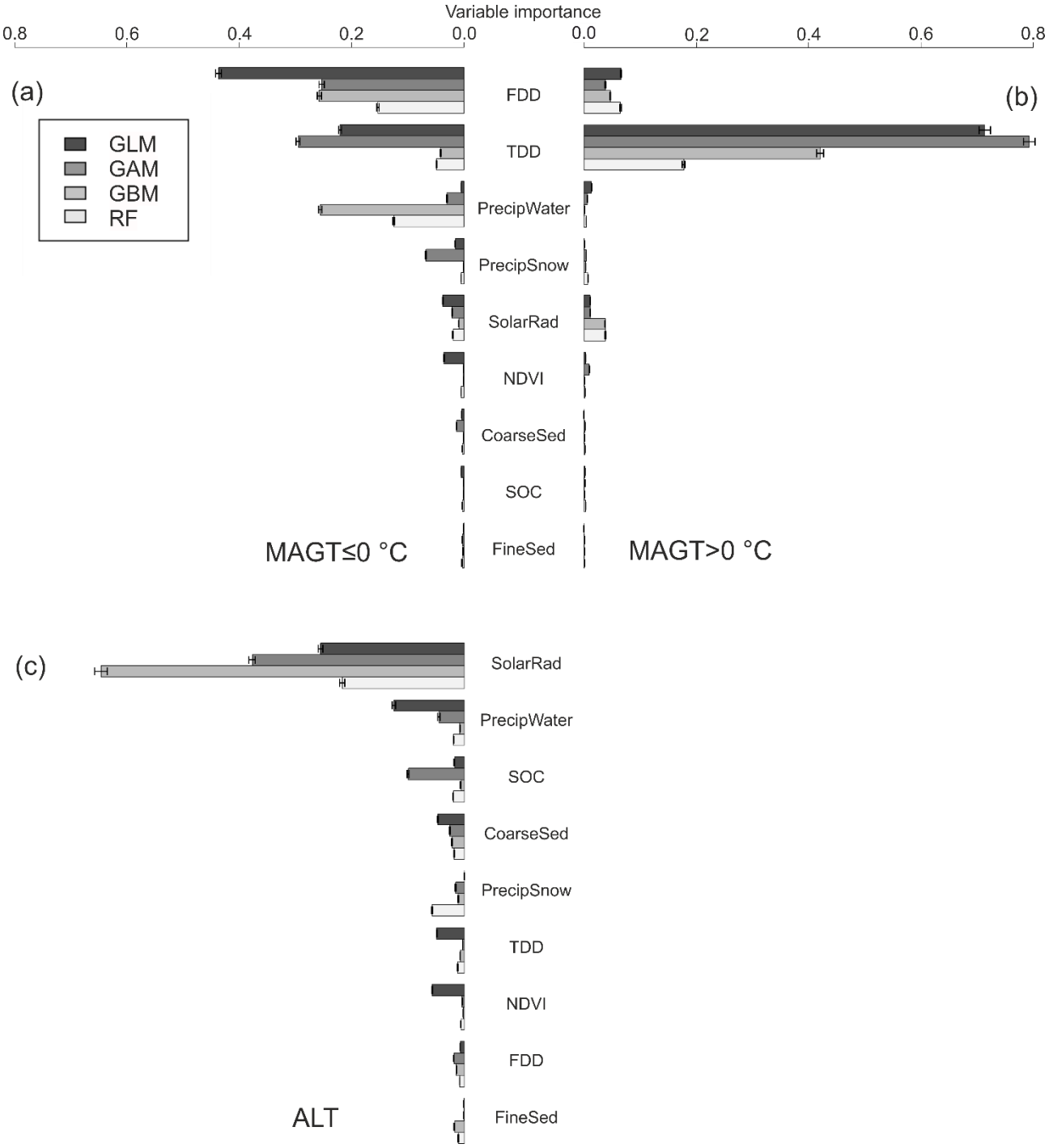

Figure 3: Variable importance values in $MAGT_{\leq 0\,°C}$ (mean annual ground temperature) (a) and $MAGT_{>0\,°C}$ (b) datasets arranged in the descending order of four-model average in $MAGT_{\leq 0\,°C}$ conditions, and for ALT (active-layer thickness) (c), arranged likewise based on ALT results. The whiskers depict 95 % confidence intervals (over 100 bootstrapping rounds). GLM = generalized linear modelling, GAM = generalized additive modelling, GBM = generalized boosting method and RF = random forest. See Sect. 2.2 for predictor abbreviations.

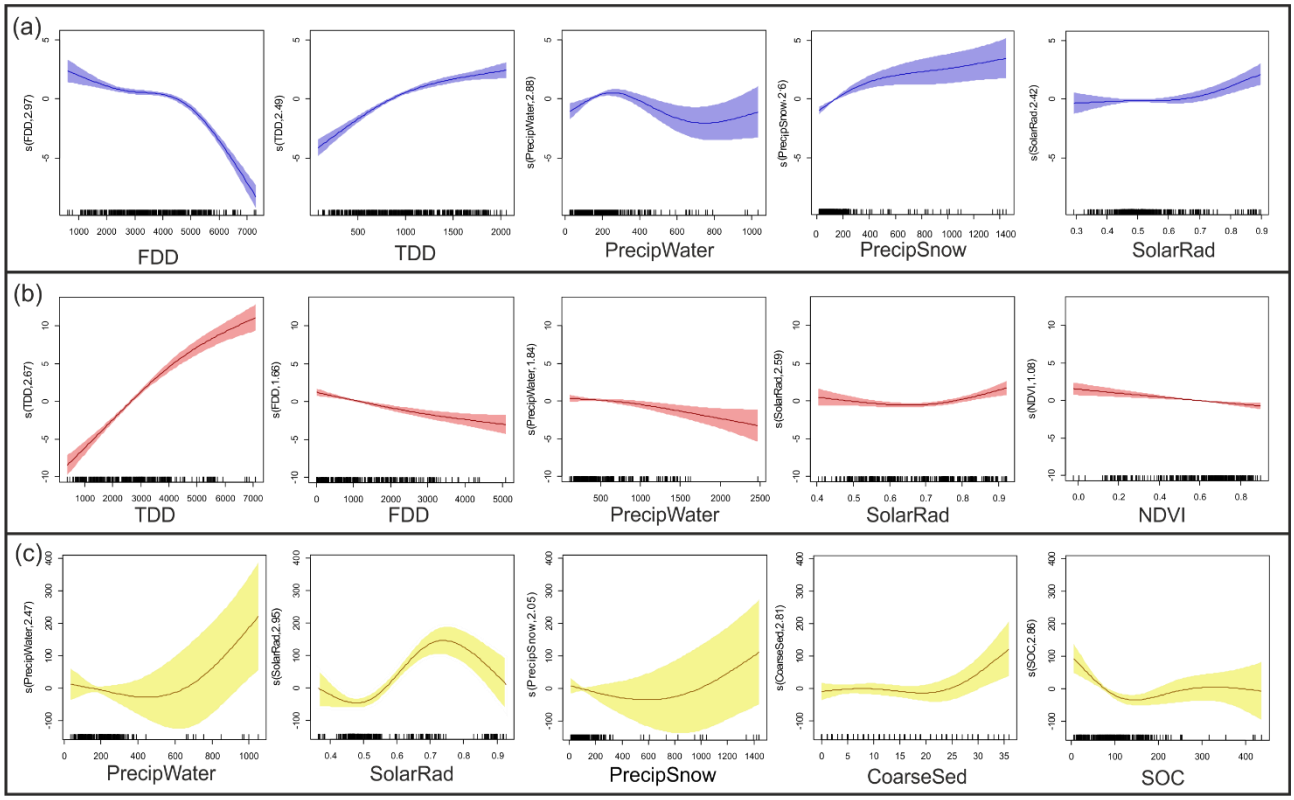

530 **Figure 4: Response shapes of the five predictors with most contribution in $MAGT_{\leq 0\,°C}$ (a) (mean annual ground temperature, blue curves), $MAGT_{>0\,°C}$ (b) (red curves) and ALT (c) (active-layer thickness, yellow curves) datasets obtained from generalized additive modelling (GAM). Response shapes for the remaining predictors are illustrated in Figure S2. Predictors (see Sect. 2.2 for abbreviations) are presented in the descending order of their effect size in respective datasets. X-axis units appear in the original scale of the predictors. Y-axis displays partial residuals and labels the estimated degrees of freedom used in fitting the respective**
535 **predictors to a response. Shaded areas depict 95 % confidence limits.**